

# Solid oxide fuel cell stacks using extruded honeycomb type elements

M. Wetzko, A. Belzner, F.J. Rohr, F. Harbach \*

*ABB Corporate Research, Speyerer Straße 4, D-69115, Heidelberg, Germany*

Received 7 January 1999; accepted 27 April 1999

## Abstract

A solid oxide fuel cell (SOFC) stack concept is described which comprises “condensed-tubes” like extruded honeycomb sections of ceramic electrolyte ( $ZrO_2$ -based) and interconnectors of nickel sheet as key elements. According to this concept, well known and extensively tested construction principles can be realised in a low-cost production. The cells are self-supported with in-plane conduction. A demonstrator model stack of five honeycomb elements and six nickel sheet seals/interconnectors was built and operated for 860 h at  $1000^\circ\text{C}$ . Volumetric power densities of  $160\text{ kW/m}^3$  were obtained with  $H_2$  vs. air, of close to  $200\text{ kW/m}^3$  with  $H_2$  vs.  $O_2$ . © 1999 Elsevier Science S.A. All rights reserved.

*Keywords:* Fuel cell; SOFC; Honeycomb; Extruded honeycomb; Demonstrator stack; Stack test

## 1. Introduction

Fuel cells are widely seen as key elements of future energy systems such as decentralised networks for electricity generation or the “hydrogen economy”. The reasons are extensively discussed in the literature:

- high conversion efficiency for electricity from chemical fuels — even at partial load conditions,
- versatility with respect to the unit size as a consequence of the modular construction principle, and
- environmental compatibility with respect to emissions and noise.

Among the various fuel cell types the solid oxide fuel cell (SOFC) has been demanding the highest effort for its development. On the other hand, the SOFC carries the highest potential with respect to fuel versatility, longevity, and life cycle costs [1]. The SOFC pilots manufactured by Westinghouse have demonstrated the technical feasibility of the SOFC, in particular of the tubular SOFC construction [2].

Other SOFC types in development are mainly of the planar–bipolar type. With a bipolar SOFC higher energy densities per volume and weight, and thus, lower capital

costs may be attained. To this aim, however, considerable technical barriers have still to be overcome. Namely sealing and electrical interconnection of bipolar SOFC stacks are much more difficult for the bipolar than for the tubular type.

The “ideal SOFC” would combine the technical simplicity and reliability of tubular SOFCs with the low-cost potential of planar bipolar SOFCs. One may accomplish this by retaining the basic topology of tubular stack constructions but translating it into planar geometries. Planar units could be realised in sizes much larger than those of SOFC cell tubes using cost effective ceramic mass production techniques such as extrusion, screen printing and others. This was the fundamental idea of an SOFC development carried out by ABB in its Heidelberg research facility from 1989 to 1993. ABB terminated its SOFC development due to a redefinition of its business strategy in power generation. This, however, does not touch the technical merits of the work completed.

Most of the development at ABB was concentrated on an SOFC construction which has been described as a planar deconvolution of a Westinghouse SOFC — the ceramic flat plate SOFC (CFP). Details of the CFP concept are given elsewhere [3]. In this paper we report a SOFC concept which is related to yet another tubular type. This is the tubular SOFC which was developed by the research group at ABB (then BBC) in an earlier effort from 1960 to 1969 [4,5]. The advanced concept which is

\* Corresponding author. Tel.: +49-6221-59-6160; fax: +49-6221-59-6253

described here was christened the “honeycomb concept” because extruded honeycombs of  $ZrO_2$  ceramics are used as equivalent to bundles of single SOFC tubes. To differentiate it from other “honeycomb concepts” it is also referred to as “condensed-tube” type honeycomb concept, because its structure can be derived from the tubular concept through a dense packing of coated tubular elements or through a condensation or a merging perpendicularly to the tubes’ axes.

## 2. Concept description

### 2.1. The tubular self supporting SOFC by BBC

In the “BBC-SOFC”, cylindrical elements of stabilised  $ZrO_2$  were employed as self supporting electrolytes with typical dimensions of 22 mm in diameter, 12 mm in length, and 0.45 mm in wall thickness. These annular elements were coated with electrode layers according to the scheme in Fig. 1, using lanthanum manganite and nickel–zirconia cermet layers as cathode and anode layers, respectively. Tubular stacks were formed by spring-loading up to 100 single cells along a common axis. The force was provided via ceramic or metallic transducer-rods by spring washers outside the hot zone of the stack.

The single cells were centred on the common axis by means of annular nickel sheet gaskets sandwiched between each two cells. These nickel-rings served as interconnection elements and sealing gaskets at the same time. They were connected tightly with the adjoining electrode layers by sintering at operation conditions (1000°C, reducing

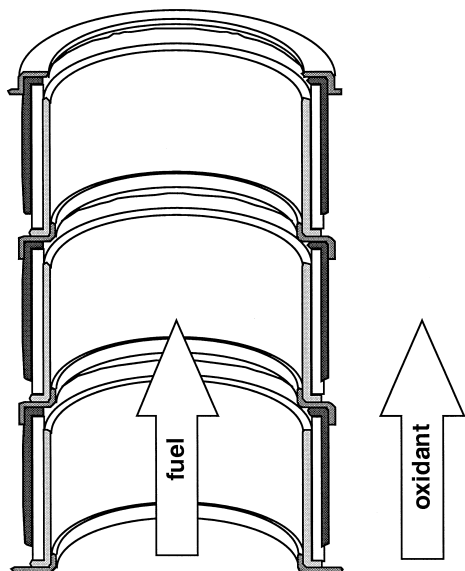


Fig. 1. “BBC-SOFC”, schematic longitudinal section of the tubular stack.

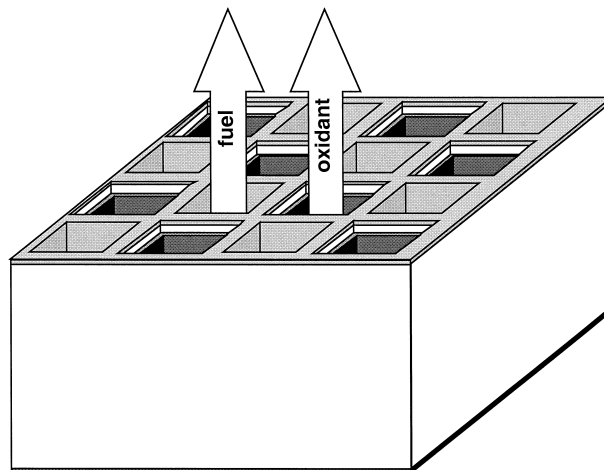


Fig. 2. Extruded honeycomb-SOFC — general assembly.

atmosphere inside the tubular stacks). Thus, the external spring force which was maintained for the entire lifetime of the stack resumed a safety and backup function only.

### 2.2. The honeycomb-SOFC

The “honeycomb-SOFC” [6] is derived from the above concept by replacing each annular electrolyte element with an extruded honeycomb section and by adapting the interconnection elements of nickel accordingly (see Figs. 2 and 3). The interior surfaces are coated with cathode or anode layers in a manner as to form a black-and-white pattern of cathode and anode channels. In the simplest case, this will be a checkerboard pattern as shown in Fig. 2. Correspondingly, the interior channels of the stack are separated into air- and fuel-channels in an alternating sequence.

Slurry coating will be the most suitable process for the application of the electrode layers. This has to be done after appropriate masking of the channel inlets, e.g., by

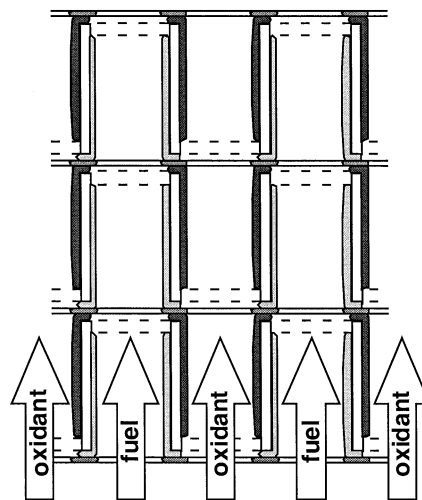


Fig. 3. Extruded honeycomb-SOFC — schematic longitudinal section.

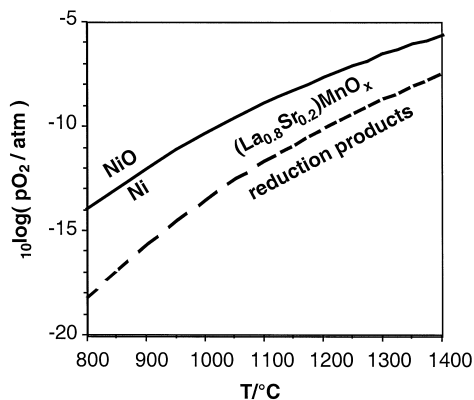


Fig. 4. Stability regimes of NiO and  $(\text{La,Sr})\text{MnO}_{3-\delta}$  as a function of temperature and oxygen partial pressure.

rubber plugs, in two subsequent coating steps. The two electrode layers can then be sintered in a single cycle.

Each internal wall element of a honeycomb section separates an air-channel from a fuel-channel. Together with the electrode layers the wall element forms a single electrochemical cell. The honeycomb section comprises already a multiple cell. The nickel gaskets act as electrical connectors — for the parallel connection of the cells within a single honeycomb section, and in addition, for the series connection of subsequent honeycomb sections in analogy to the tubular construction. The first and the last nickel elements of each stack are used as the external electrical terminals.

The gas manifolds at the inlet ends of the stacks (bottom) can be fashioned from ceramic plates (at least three) with adapted bore patterns. The plates are joined by glass or again by metal gaskets to a “stack” in the literal sense. This, at least, was the solution adopted for a lab test module — see below. Here, the same type of manifold was used at the outlet of the stack, since the lab-setup did not incorporate an afterburner zone at the outlet on top of the stack.

In technical size units, it will be more feasible to extend the inlet side of the stack into the cold zone of the unit by accordingly long honeycomb sections without electrode layers. These terminal sections serve as force transducers and gas supply channels. In this case, metallic parts and polymer seals may be used for the manifolding.

### 2.3. The nickel interconnector

The application of metallic nickel as interconnector material (ICM) was adapted for the honeycomb-SOFC as a crucial feature of the earlier tubular concept. Commonly, lanthanum chromites ( $\text{LaCrO}_{3-\delta}$  with various additives) are employed as ICM because these are the only materials which, at SOFC temperatures, are stable in air as well as in the fuel atmosphere while maintaining sufficient electrical conductivity.

Lanthanum chromites are expensive and technically difficult to handle. Generally, chromite ceramics of sufficient density are obtained only by sintering at conditions which in terms of temperature and oxygen partial pressure are not easily compatible with the other stack components. Moreover, lanthanum chromites tend to react with zirconia based ceramics and with sealing and bonding materials containing silica. Major technical headaches in the course of SOFC-developments have been related to the implementation of lanthanum chromites as ICM.

Nickel does not readily offer itself as a replacement for lanthanum chromites because it is not stable in air. At SOFC-operating temperatures, it is quickly oxidised to NiO which is a poor conductor. In an arrangement as shown in Figs. 1 and 3 however, the bulk of the nickel is protected against oxidation by solid state hydrogen diffusion from the fuel compartment.

Similarly, the layer of cathode material extending into the fuel compartment will be reduced to a certain depth. At this depth, a further reduction is prevented by the diffusion of oxygen from the air compartment. In both, nickel ICM as well as extended cathode layer, the position of the “reduction front” is determined by the relative diffusion velocities of  $\text{H}_2$  and  $\text{O}_2$  in the materials and by the chemical stability of the materials. Here, it comes into effect that lanthanum manganite is actually quite stable against reduction. The stability regimes of metallic nickel and  $\text{LaMnO}_{3-\delta}$  as a function of the oxygen partial pressure overlap [7,8] (see Fig. 4). In an arrangement as realised in the nickel interconnection, this will lead to a geometrical overlap of metallic nickel and unreduced  $\text{LaMnO}_{3-\delta}$  which provides electrical conduction paths.

The technical application of this interconnection principle requires the non-functional parts of cathode and nickel layers, in particular the reduced part of the cathode, to remain mechanically stable enough as to stay in place and serve as gas diffusion barriers. This was verified for the presently used combination of materials in the course of the work on the tubular BBC-SOFC. Stacks of the order of 100 W in maximum power yielded a stable performance for operation times of up to 20,000 h, an interconnected

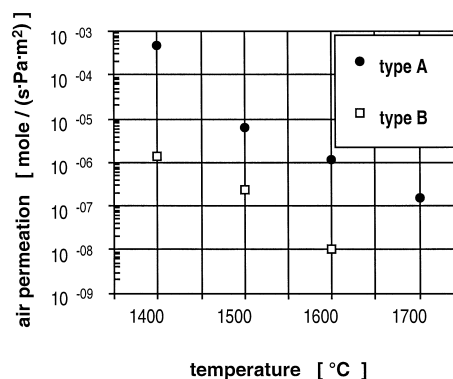


Fig. 5. Pressure decay in various  $\text{ZrO}_2$  electrolyte honeycomb sections.

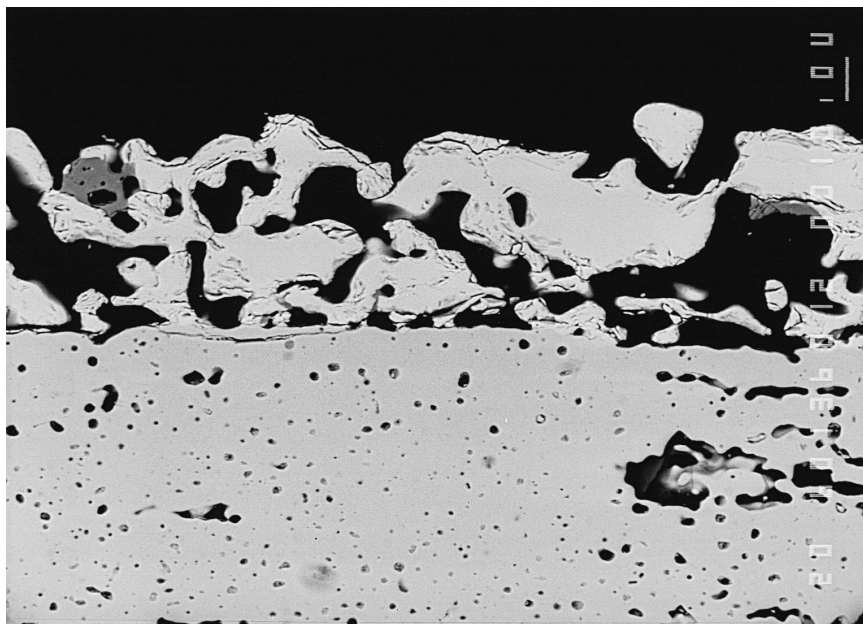


Fig. 6. Ceramographic cross section of brush coated cathode layer, directly after sintering, SEM, backscattered electrons (composition contrast).

single cell (short stack) for even 50,000 h. These long term tests included thermal cycling [3,4].

During these tests, it was also shown that the loss of fuel by diffusion of hydrogen through the nickel interconnectors did not exceed some 2% while losses due to incomplete fuel utilisation were in the order of 10 to 15% [4].

It should be noted that the planar bipolar SOFC type does not allow an interconnection with nickel, because in this SOFC type a controlled diffusion of gases along the

interconnection cannot be realised. For the honeycomb concept, however, the nickel interconnection offers itself as a well proven and very cost effective solution.

### 3. Honeycomb-SOFC demonstrator tests

A demonstrator model for the honeycomb concept was built and successfully operated. Due to the termination of

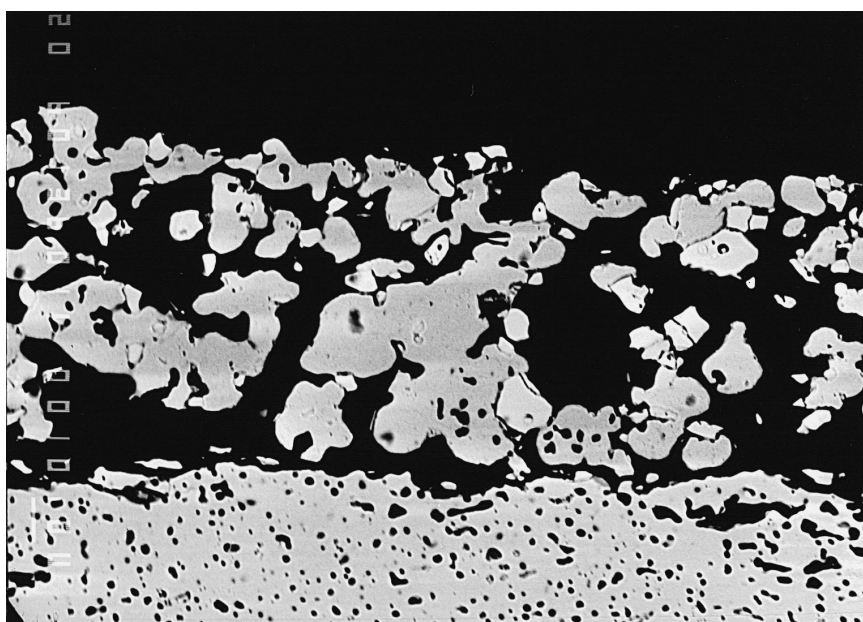


Fig. 7. Ceramographic cross section of brush coated anode layer, directly after sintering, SEM, backscattered electrons (composition contrast).

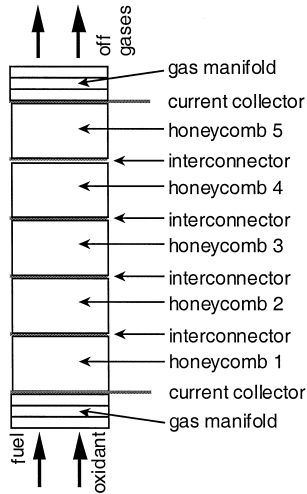


Fig. 8. Honeycomb concept demonstrator — schematic assembly.

the SOFC-project of ABB, this was restricted to the lab-scale. One should view the results below not as a final state but rather as potential starting point of a promising development.

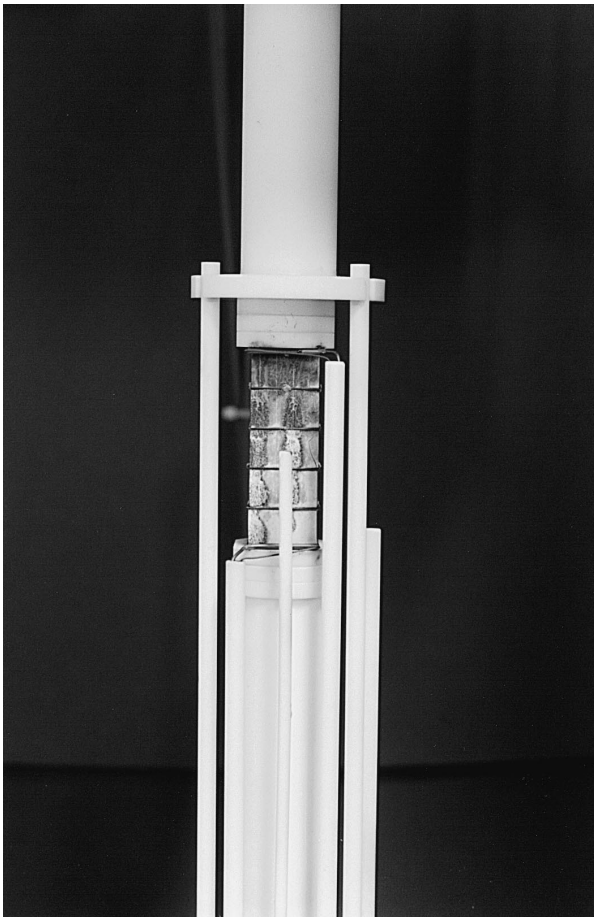


Fig. 9. Honeycomb concept demonstrator — stack in test rig.

### 3.1. $ZrO_2$ — honeycombs

Extrusion and sintering tests were performed with two types of zirconia powder: yttria stabilised zirconia ( $ZrO_2/8\% Y_2O_3$  per mole) with median grain sizes  $d_{50}$  of  $3 \mu\text{m}$  (type A) and  $0.5 \mu\text{m}$  (type B). Both powder types were processed to extrudable ceramic masses without additives containing alkalines or silicon.

An extrusion dye for catalyst production was used which had not been optimised for the present application. The die comprised  $4 \times 4$  quadratic cells with a cell pitch of  $6 \text{ mm}$  and a thickness of  $700 \mu\text{m}$  for the internal cell walls. Extruded pieces were cut into sections after drying and then sintered.

Sintering tests were performed with peak temperatures of  $1400^\circ\text{C}$  to  $1700^\circ\text{C}$  with a soak time of 2 h each. After sintering, the gas permeabilities were measured with a pressure decay method using air at  $20^\circ\text{C}$ . A dense ceramic was obtained only with the fine powder (type B) by sintering at  $1700^\circ\text{C}$ . In all other cases, a gas pressure decay was observed, though decreasing with increasing sintering temperature (see Fig. 5).

The fine powder (type B) gave the better results concerning density and structure of the sintered ceramics. The



Fig. 10.

powder type A was superior with respect to sintering yield and dimensional accuracy. This is due to the lower shrinkage rates of the coarser type A material. Processing of type B powders had not been optimised with respect to the deagglomeration of the powder and according high density of the green compact. (Efficient methods for deagglomeration and processing of fine powders as described in Refs. [9,10] had not yet been applied for production of ceramic specimens used for these investigations.)

For the present demonstration test only type A honeycombs were used. These were sintered at 1730°C with a soak time of 5 h. A gas permeation of less than  $5 \times 10^{-8}$  mol/(s Pa m<sup>2</sup>) was attained. The sintered honeycomb sections were about 12 mm in length with a cell pitch of 5.1 mm, free channel widths of 4.5 mm and internal walls of 0.55 to 0.65 mm in thickness.

### 3.2. Electrode layers

Lanthanum manganite (La<sub>0.84</sub>Sr<sub>0.16</sub>)MnO<sub>x</sub> and nickel–zirconia cermet were used for cathode and anode, respectively. The cathode material was prepared by solid state reaction of the starting oxides (SrO as SrCO<sub>3</sub>), the anode material by calcining a mixture of NiO and yttria stabilised

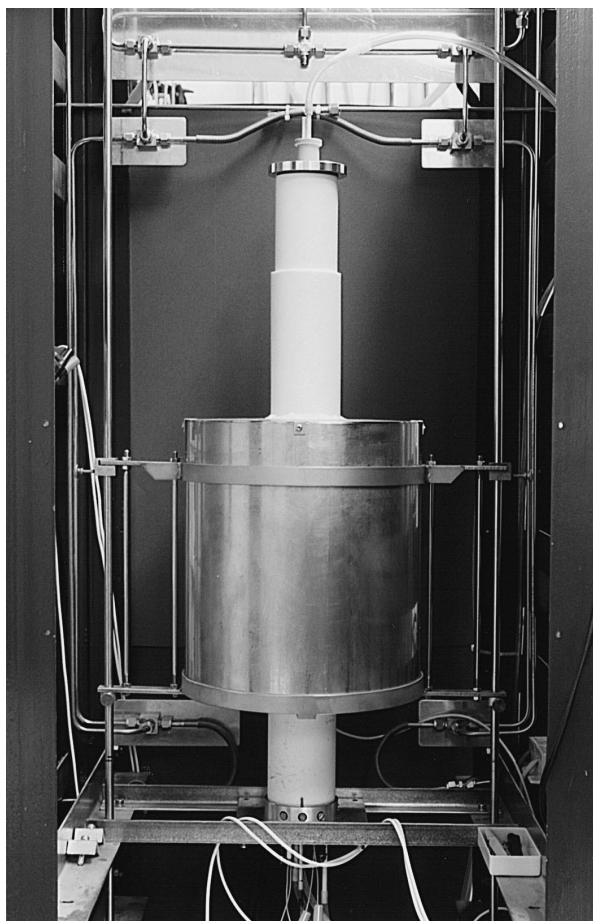


Fig. 11.

Table 1  
SOFC stack, five honeycombs — performance data at 1000°C with H<sub>2</sub>-fuel

	Oxidant	
	Air	Pure O <sub>2</sub>
Open-circuit voltage per cell (V)	1.09	1.12
Maximum power (W)	4.2	5.1
Maximum power density per active area (kW/m <sup>2</sup> )	0.99	1.2
Maximum power density per stack volume (kW/m <sup>3</sup> )	160	190

zirconia (8 mol%). The finally calcined materials were crushed and ground. Grain fractions > 60 μm were removed by a mesh screen before the material was dispersed in an organic carrier system. Details of the material preparation are given in Ref. [11].

Slurry coating is seen as the most suitable process for the application of the electrode layers. For the present demonstration test, the ZrO<sub>2</sub> honeycombs were manually brush coated with the electrode dispersions. By inserting rubber plugs into the proper end of each channel, the terminating channel sections were kept free of electrode material.

After drying both electrode layers were fired simultaneously at 1550°C in air. Ceramographic cross-sections of the sintered electrode layers are shown in Figs. 6 and 7.

### 3.3. Stack assembly and testing

After successful testing of single honeycomb sections a stack according to the description in Section 2.2 was assembled and operated. The stack comprised five honeycomb elements and six nickel sheet seals/interconnectors each 0.1 mm thick. Alumina ceramics was used for the pressure transducer rods and the gas manifolds on bottom and on top of the stack. A schematic drawing of the assembly is shown in Fig. 8. Figs. 9–11 are photographs of the stack and the entire setup including the test furnace.

Hydrogen (H<sub>2</sub>) was used as fuel and air or pure oxygen (O<sub>2</sub>) as oxidant. The stack was heated up to 1000°C at a rate of 10 K/h while the air compartment was flushed

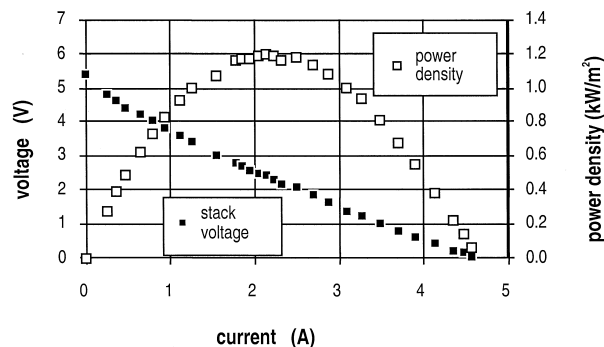


Fig. 12. Honeycomb demonstrator test —  $U/I$ -curves at optimum performance, 1000°C, H<sub>2</sub> (55 l/h) vs. O<sub>2</sub> (80 l/h), five honeycombs in series, total dimensions 21 × 21 × 60 mm<sup>3</sup>.

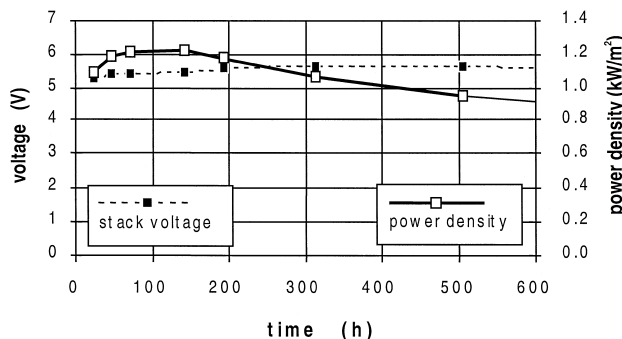


Fig. 13. Honeycomb demonstrator test — performance as a function of time, 1000°C, H<sub>2</sub> vs. O<sub>2</sub>.

with air and the fuel compartment with a mixture of 95% N<sub>2</sub> and 5% H<sub>2</sub>. This way, the NiO in the anode layers was reduced carefully to elementary nickel.

A total operation time of 860 h at 1000°C was attained. The optimum performance data were measured after ca. 100 h of operation and are given below in Table 1. A voltage/current curve for H<sub>2</sub>/O<sub>2</sub> is shown in Fig. 12.

For cost effective power generation, power densities of more than 1 kW/m<sup>2</sup> per active area are required. This limit was met closely enough for a “first shot” experiment.

The comparatively low open-circuit voltage for air operation indicates that there is still a leakage problem. As stated above, for this demonstrator model a ZrO<sub>2</sub>-electrolyte with some open porosity was accepted. For the long term operation pure oxygen was used as oxidant. As shown in Fig. 13, there is a power decay of ca. 20% within a total operation time of 860 h. Most probably this is also due to hydrogen leakage across the electrolyte which deteriorates the cathode layer and the cathode/electrolyte interface.

## 4. Discussion

### 4.1. Electrical performance prospects

Neither honeycomb geometry nor electrolyte material were optimised for the tests reported here. In particular, the thickness of the walls should be decreased from presently 550 to 650 μm to values below 400 μm [12]. At the same time, the gas tightness of the ZrO<sub>2</sub> electrolyte needs to be improved. This seems not too difficult for lab-scale demonstration problems. The challenge for a product development is to compromise this with processing requirements for a large scale production.

A large optimisation potential for the electrode layers can also be derived, from current literature as well as from the experiences with tubular stacks. Based on the latter a power density of more than 2 kW/m<sup>2</sup> active area should be attainable with air as oxidant. A module consisting of

100 honeycomb sections of each 6 × 6 cells with overall dimensions of 6 × 6 × 12 cm<sup>3</sup> in the active part should be able to provide a power of 1 kW, i.e., 230 kW/m<sup>3</sup>.

### 4.2. Security, reliability, durability

Single honeycomb stacks can, in principle, simply be bundled to form larger units. One can also leave spaces between the single honeycombs for cooling or purging gas. This way, additional technical security may be introduced on the expense of the volumetric power density. It is, for instance, always possible in a honeycomb-SOFC to avoid overheating of large stacks without increasing the air to fuel ratio.

A high degree of intrinsic electrical reliability is secured by the high degree of electrical cross connection of the single cells. Honeycomb stacks are, in particular, tolerant vs. single cell failures by open circuit. In this respect, they compare favourably with bipolar stacks which are entirely set out of function by a single open-circuit failure.

Additional inherent reliability is given by the option to locate the gas manifolding entirely outside of the hot parts of a unit. There is no need to deal with complicated ceramic parts, joints or seals in the hot zones. The only joints in the hot parts of the stack are the nickel gaskets, and these have been proven to work reliably over periods in the order of 50,000 h — see above. This holds also for the other principal components of the cell.

### 4.3. Cost perspectives

With respect to mass production costs, the honeycomb cell should be in favour with respect to the Westinghouse cell for two reasons:

- The material usage per active cell area is significantly reduced.<sup>1</sup>
- The lengthy and expensive EVD processes are eliminated.

In comparison to bipolar SOFCs, the elimination of expensive materials such as lanthanum chromite and/or high temperature alloys is also in favour of the honeycomb type. Extrusion and sintering of honeycomb elements should be possible at costs per active area which are comparable to those of tape cast electrolyte foils. On the other hand, the material usage per output power will be higher, and the coating of the electrodes is somewhat more complicated, thus, more expensive.

The immediate advantage of the honeycomb vs. bipolar SOFCs is given by its inherent simplicity and reliability as well as by its comparatively low development risk. State and prospects of this fuel cell type do certainly warrant a further evaluation.

<sup>1</sup> Thick layers of either ZrO<sub>2</sub> or cathode material for cell support are eliminated as well as the need for ZrO<sub>2</sub> air inlet tubes.

## References

- [1] J. Meusinger, L.G.J. de Haart, Stand der oxidkeramischen SOFC-Technik, in: *Energieversorgung mit Brennstoffzellenanlagen '98: Stand und Perspektiven*, VDI-Bericht 1383, Verein Deutscher Ingenieure, VDI-Gesellschaft Energietechnik, VDI-Verlag, Düsseldorf, 1998, p. 61.
- [2] S.C. Singhal, Recent Progress in Tubular Solid Oxide Fuel Cell Technology, in: U. Stimming, S.C. Singhal, H. Tagawa, W. Lehnert (Eds.), *Proc. of the 5th Int. Symposium on Solid Oxide Fuel Cells (SOFC-V)*, Vols. 97–40, The Electrochem. Soc., Pennington, NJ, 1997, p. 37.
- [3] R.F. Singer, F.J. Rohr, A. Belzner, Solid oxide fuel cells: CFP design and cell performance, in: *Fuel Cell Seminar, Proc. 1990*, pp. 111–114.
- [4] F.J. Rohr, High Temperature Fuel and Electrolysis Cells With Zirconia Solid Electrolytes, in: T. Takahashi, A. Kozawa (Eds.), *Applications of Solid Electrolytes*, JEC Press, Cleveland, OH, 1980, pp. 196–205.
- [5] H. Holich, H. Kleinschmager, R. Krapf, A. Minor, F.J. Rohr, Entwicklung des Prototypen einer Hochtemperatur-Brennstoffzellen-Batterie, Brown Boveri and Cie AG; Project with the German Federal Department for Research and Technology, Final Report No. NT-332, February 1976.
- [6] F.J. Rohr, A. Reich, N. Pfeifer, Brennstoffzellenmodul und Verfahren zu seiner Herstellung, European Patent EP 0503526 (09.03.1992).
- [7] J. Mizusaki, H. Tagawa, K. Naraya, T. Sasamoto, Nonstoichiometry and thermochemical stability of the perovskite-type  $\text{La}_{1-x}\text{Sr}_x\text{MnO}_{3-\delta}$ , *Solid State Ionics* 49 (1991) 111–118.
- [8] I. Barin, *Thermochemical Data of Pure Substances: Part II*, VCH, Weinheim, 1989, p. 1067.
- [9] F. Harbach, J. Nienburg, Homogeneous functional ceramic components through electrophoretic deposition from stable colloidal suspensions: I. Basic concepts and application to zirconia, *J. Eur. Ceram. Soc.* 18 (1998) 675–683.
- [10] F. Harbach, J. Nienburg, Homogeneous functional ceramic components through electrophoretic deposition from stable colloidal suspensions: II. Beta-alumina and concepts for industrial production, *J. Eur. Ceram. Soc.* 18 (1998) 685–692.
- [11] A. Belzner, F.J. Rohr, G.R. Heath, F. Harbach, K. Kendall, C. Bagger, M. Mogensen, J. Gerretsen, A. Mackor, *New Manufacturing Technologies for Advanced Solid Oxide Fuel Cells*, Final Technical Report, BRITE-EURAM Contract No. BREU-0185-C (MB), April 1993.
- [12] F.J. Rohr, Brennstoffzellenmodul, German Patent Application P 43 00 520.9 (12.01.1993).